

should eventually make it possible to unravel all the parameters involved in the leptonic decay.

Fortunately, it turns out that the most direct measurement of the K_1-K_2 mass difference is independent of the question of either *CPT* or *CP* invariance. On the other hand, the test of the $\Delta S = \Delta Q$ rule based on leptonic decay rates of K^0 mesons does depend on these questions so that there exists an ambiguity in the interpretation of the presently available experimental data. However, a more accurate determination of the

charge asymmetry in these decay processes will serve to resolve the ambiguity.

ACKNOWLEDGMENTS

The author would like to thank Dr. Motchane, and Professor L. Michel for the hospitality extended to him by the Institut des Hautes Études Scientifiques, Paris, and to Professor Abdus Salam for the hospitality extended to him at the Physics Department, Imperial College, London.

K^+-p and K^-p Total Cross Sections in the Momentum Range 3–19 BeV/c*

W. F. BAKER, R. L. COOL, E. W. JENKINS, T. F. KYCIA, R. H. PHILLIPS, AND A. L. READ

Brookhaven National Laboratory, Upton, New York

(Received 31 October 1962)

The total cross sections of K^+ and K^- mesons on protons have been measured between 3 and 19 BeV/c at the Brookhaven alternating gradient synchrotron. The data were obtained from measurements of attenuation in a liquid hydrogen target. The K mesons were defined in momentum by magnetic deflection and a scintillation counter telescope. They were identified by measuring the velocity with a high-pressure gas-filled Čerenkov counter. Values of the cross sections were obtained at intervals of ~ 1 BeV/c with an error for each value of approximately 5%. $\sigma_t(K^+p)$ is, within errors, constant over the entire momentum range with a value of 18.4 mb. $\sigma_t(K^-p)$ decreases gradually from a value of 28 mb at 4 BeV/c to 21.6 mb at 19 BeV/c. The cross sections are significantly different up to the highest momenta reached in this experiment.

I. INTRODUCTION

THE successful operation of proton accelerators in the 30-BeV range at CERN and at the Brookhaven National Laboratory has made it possible to increase substantially the energy range of total cross-section measurements. We report here measurements of total cross sections of K^+ and K^- mesons on protons between 3 and 19 BeV/c at the Brookhaven alternating gradient synchrotron (AGS). At momenta below 5 BeV/c, data have been published by a number of authors.^{1–10} More recently some data above 5 BeV/c have been reported from the CERN laboratory.^{9,10}

Advances in the theory of strong interactions have given added impetus to attempts to extend cross-section measurements to the highest available energies. On the basis of general field-theoretical arguments, Pomeranchuk¹¹ has shown that, in the high-energy limit, particle and antiparticle total cross sections should become equal. More recently Chew and Frautschi¹² have proposed that the elastic scattering amplitude for any process is dominated by the Regge pole¹³ in the crossed channel. Within this framework, Udgaonkar¹⁴ has shown that it may be possible to understand how the different cross sections approach the Pomeranchuk limit.

In Secs. II and III we describe the apparatus and

* Work done under the auspices of the U. S. Atomic Energy Commission.

¹ For a summary of early K meson-proton total cross sections at low momenta, see V. S. Barashenkov, and V. M. Maltsev, *Fortschr. Physik* **9**, 549 (1961).

² T. F. Stubbs, H. Bradner, W. Chinowsky, G. Goldhaber, S. Goldhaber, W. Slater, D. H. Stork, and H. K. Ticho, *Phys. Rev. Letters* **7**, 188 (1961).

³ O. Chamberlain, K. M. Crowe, D. Keefe, L. T. Kerth, A. Lemonick, Tin Maung, and T. F. Zipf, *Phys. Rev.* **125**, 1696 (1962).

⁴ S. Goldhaber, W. Chinowsky, G. Goldhaber, W. Lee, T. O'Halloran, T. F. Stubbs, G. M. Pjerrou, D. H. Stork, and H. K. Ticho, *Phys. Rev. Letters* **9**, 135 (1962).

⁵ H. C. Burrows, D. O. Caldwell, D. H. Frisch, D. A. Hill, D. M. Ritson, and R. A. Schluter, *Phys. Rev. Letters* **2**, 117 (1959).

⁶ A. S. Vovenco, B. A. Kulakov, M. F. Lykhachev, A. L. Ljubimov, Ju. A. Matulenko, I. A. Savin, Ye. V. Smirnov, V. S. Stavinsky, Sui Yuin-chan, and Shzan Nai-sen, The Joint Institute for Nuclear Research, Dubna Report D721, May, 1961 (unpublished), and *Proceedings of the 1962 Annual International*

Conference on High-Energy Physics at CERN (CERN, Geneva, 1962), p. 385. M. F. Lykhachev, V. S. Stavinsky, Hsü Yün-ch'ang, and Chang Nai-sen, *J. Exptl. Theoret. Phys. (U.S.S.R.)* **41**, 38 (1961) [translation: *Soviet Phys.—JETP* **14**, 29 (1962)].

⁷ V. Cook, D. Keefe, L. T. Kerth, P. G. Murphy, W. A. Wenzel, and T. F. Zipf, *Phys. Rev. Letters* **7**, 182 (1961).

⁸ V. Cook, B. Cork, T. F. Hoang, D. Keefe, L. T. Kerth, W. A. Wenzel, and T. F. Zipf, *Phys. Rev.* **123**, 320 (1961).

⁹ G. von Dardel, D. H. Frisch, R. Mermod, R. H. Milburn, P. A. Piroué, M. Vivargent, G. Weber, and K. Winter, *Phys. Rev. Letters* **5**, 333 (1960).

¹⁰ G. von Dardel, R. Mermod, P. A. Piroué, M. Vivargent, G. Weber, and K. Winter (to be published); quoted by A. M. Wetherell in *Rev. Mod. Phys.* **33**, 382 (1961).

¹¹ S. Pomeranchuk, *Zh. Eksperim. i Teor. Fiz.* **34**, 725 (1958) [translation: *Soviet Phys.—JETP* **7**, 499 (1958)].

¹² G. F. Chew and S. C. Frautschi, *Phys. Rev. Letters* **7**, 394 (1961); **8**, 41 (1962).

¹³ T. Regge, *Nuovo Cimento* **14**, 951 (1959); **18**, 947 (1960).

¹⁴ B. M. Udgaonkar, *Phys. Rev. Letters* **8**, 142 (1962).

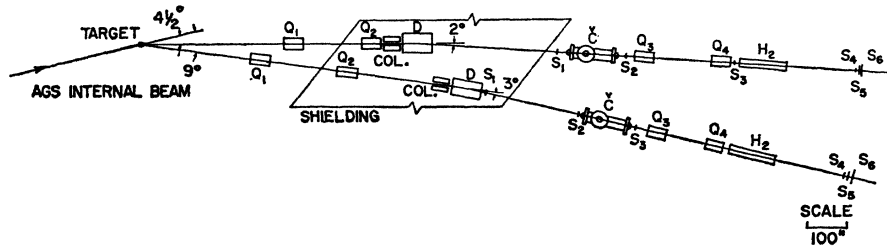


FIG. 1. Beam layouts for $K^\pm p$ total cross-section measurements. K mesons were produced at the Brookhaven AGS in an internal target. The $4\frac{1}{2}^\circ$ beam was used for measurements from 10 to 19 BeV/c, and the 9° beam for measurements from 3 to 12 BeV/c.

experimental procedure in some detail. The results appear in Sec. IV, and they are compared with other measurements and the theoretical predictions in Sec. V.

II. APPARATUS

A. Beam

A schematic layout of magnets, collimators, counters, and target is shown in Fig. 1. The beam produced at an angle of 4.5° with respect to the circulating proton-beam direction was used for measurements at momenta between 10 and 19 BeV/c; a similar arrangement at 9° was used in the 3 to 12 BeV/c range. The K mesons were produced within an area of ~ 1 cm diameter in internal targets of various materials (C, CH_2 , Be, and Al) according to availability. The deflection magnet (D), the counter telescope ($S_1S_2S_3$), the collimator (COL), and the target defined the beam. The dimensions and locations of the collimator, the counter S_2 , and the deflection magnet (D) determined the momentum of the beam. The momentum spread $\Delta p/p$ varied between $\pm 1.2\%$ at 3 BeV/c and $\pm 2.0\%$ at 19 BeV/c.

Although the target was located in a region of negligible magnetic field, the trajectories of the 4.5° beam particles passed through a region of appreciable fringing field from the synchrotron magnet. The resulting deflection caused the particles to enter at an angle with respect to the initial axis of the system. Moreover, this angle was magnified by the quadrupoles Q_1 and Q_2 . The mean momentum was reduced for positive particles by roughly 1 BeV/c and similarly was increased for nega-

tive particles, with respect to the values expected for particles entering the system along the quadrupole axes. The momentum values for the 4.5° beam quoted below have been corrected for this effect^{15,16}; no correction was required for the 9° beam.

A schematic representation of the beam optics is shown in Fig. 2. The quadrupole doublet Q_1Q_2 produces a nearly parallel beam in both the horizontal and vertical planes. After passing through the Čerenkov counter C (Fig. 1), the quadrupole doublet Q_3Q_4 refocuses the beam into an image at the final counters ($S_4S_5S_6S_7$). The system accepted particles within a solid angle of approximately 10^{-5} sr.

The somewhat unusual beam optics was dictated by two important experimental considerations. First, the velocity-sensitive differential Čerenkov counter C , described in the following section, has a very small angular acceptance. At 20 BeV/c it counts with full efficiency only those particles within $\pm 7 \times 10^{-4}$ rad; at lower momenta, say 10 BeV/c, this requirement can be reduced somewhat but is still only $\pm 2 \times 10^{-3}$ rad. Thus, the beam produced by Q_1Q_2 had to be parallel within the above tolerances to be counted with full efficiency. Second, a sharp focus at the final counters ($S_4S_5S_6S_7$) was desired in order to minimize the correction in extrapolating the measured cross section to zero angle. At these momenta, most of the diffraction scattering from a proton is confined within an angle of a few degrees (e.g., at 20 BeV/c within $\sim 2.5^\circ$). A more detailed discussion on this point will be given in Sec. IV.

B. Čerenkov Counter

The selection of K mesons, and the rejection of particles of different mass but equal momentum within the beam, was accomplished by the gas-filled differential Čerenkov counter C .¹⁷ A diagram of the optical system of this counter is given in Fig. 3. The counter is designed such that Čerenkov radiation emitted in a small cone

¹⁵ The effect of the fringing field of the AGS on the trajectories of secondary particles produced at the internal target at G10 has been calculated by the IBM-704 program BEAM, written by E. D. Courant, Brookhaven National Laboratory Accelerator Department Internal Report EDC-36 (unpublished).

¹⁶ Using the output of Courant's IBM-704 program the momentum shift was calculated as a function of selected momentum using the IBM-704 program written by W. F. Baker, Accelerator Department Internal Report WFB-1 (unpublished).

¹⁷ T. F. KyCIA and E. W. Jenkins, Nucl. Electron. 1, 63 (1962) [Proceedings of the International Atomic Energy Agency Conference on Nuclear Electronics, Belgrade, Yugoslavia, 1961] 724.

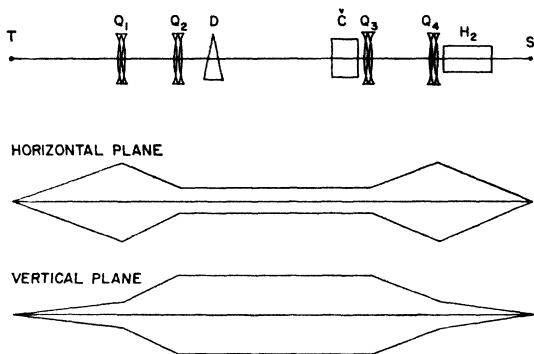
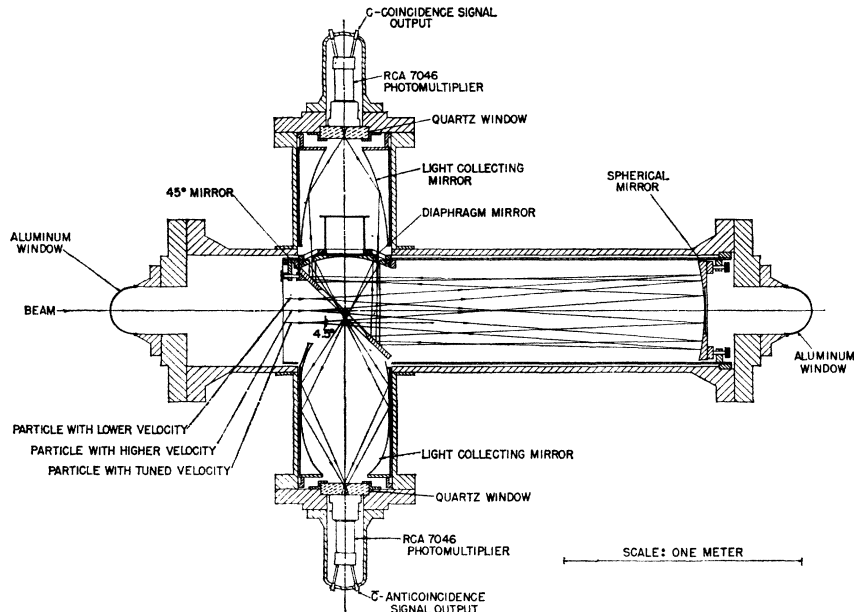


FIG. 2. Schematic diagram of beam optics for focusing particles from the AGS target, T , onto the final counters, S . The effect of the deflection magnet, D , is not shown.

FIG. 3. Čerenkov counter optical system.



about a fixed angle of 4.5° is focused by a spherical mirror into a ring image at an annular slit. The Čerenkov light which passes through this defining aperture is focused upon a 5-in.-diam photomultiplier tube (RCA 7046). The defining annular slit itself is cut into an ellipsoidal mirror. Light which arrives outside the slit is refocused by this mirror onto another 5-in.-diam photomultiplier tube. The signal-to-noise ratio is improved by requiring, with tunnel-diode discriminators, a large pulse from the light passing through the slit (the coincidence channel C) and only a small pulse from the light which appears outside it (the anticoincidence channel \bar{C}). Typically the background due to knock-on electrons, off-axis and off-momentum particles, and other sources is reduced by more than an order of magnitude in this way.

The counter is filled with CO_2 gas and can be operated at pressures as high as 1000 psig. The CO_2 radiator is 2.5 m in length and 18 cm in useful diameter. It yields at least 25 photoelectrons in the coincidence channel. A range of relative velocities $\beta = v/c$ from 0.98 to 1.0 is covered by varying the gas pressure and thus the index of refraction according to the relation $\cos\theta = 1/n\beta$, where n is the index of refraction and θ is the Čerenkov angle which is fixed at 4.5° .

The counter is designed to resolve particles whose relative velocities differ by as little as $\Delta\beta = 2 \times 10^{-4}$ at momenta greater than 18 BeV/c. An example of a resolution curve at a momentum of 18 BeV/c is shown in Fig. 4; the velocity difference between the K^+ and π^+ peaks correspond to $\Delta\beta = 3.6 \times 10^{-4}$. In the momentum range of a few BeV/c, multiple scattering in the counter windows and gas appreciably broadens the ring image. The width of the annular slit can be changed to accommodate the full image size.

C. Electronics

Figure 5 is a block diagram of the electronics. The transistorized coincidence circuits, discriminators (DISC), and fanouts were designed by Sugarman *et al.*¹⁸ The discriminator makes use of 20-mA tunnel diodes (Z 61-22), and its operation is stable for input pulses from 2 to 20 mA.

The counters ($S_4S_5S_6S_7$) were circular plastic scintillators 0.5 in. thick of various diameters. They were viewed by RCA 6810 A photomultiplier tubes. The high voltage was supplied at each tube base by a radio-frequency oscillator, transformer, and rectifier.¹⁸ The outgoing pulses were limited at the tube base to ~ 6 mA.

The coincidences ($S_1S_2S_3$) and ($S_1S_2S_3\bar{C}\bar{C}$) were recorded. ($S_1S_2S_3$) gives the total number of charged particles; ($S_1S_2S_3\bar{C}\bar{C}$) gives the number of particles of the selected mass value (e.g., K mesons). The final counters $S_4S_5S_6$ were of graduated sizes with S_4 the smallest, S_6 the largest. Their purpose was to obtain the variation of the total cross section measured at different small angle cutoffs in order to extrapolate to zero angle. For this purpose the coincidences ($S_1S_2S_3\bar{C}\bar{C}S_4$), ($S_1S_2S_3\bar{C}\bar{C}S_5$), and ($S_1S_2S_3\bar{C}\bar{C}S_6$) were recorded. Since, according to the optical model, the width of the diffraction peak is inversely proportional to the momentum, the sizes of counters S_4 , S_5 , and S_6 were selected as appropriate to the momentum.

During the experiment the internal targeting conditions were sometimes erratic which gave large variations

¹⁸ R. Sugarman, W. A. Higinbotham, F. C. Merritt, and A. H. Yonda, Brookhaven National Laboratory Report BNL-5390 (unpublished); R. M. Sugarman and W. A. Higinbotham, *Proceedings of the International Conference on Instrumentation for High-Energy Physics* (Interscience Publishers, Inc., New York, 1961), p. 54.

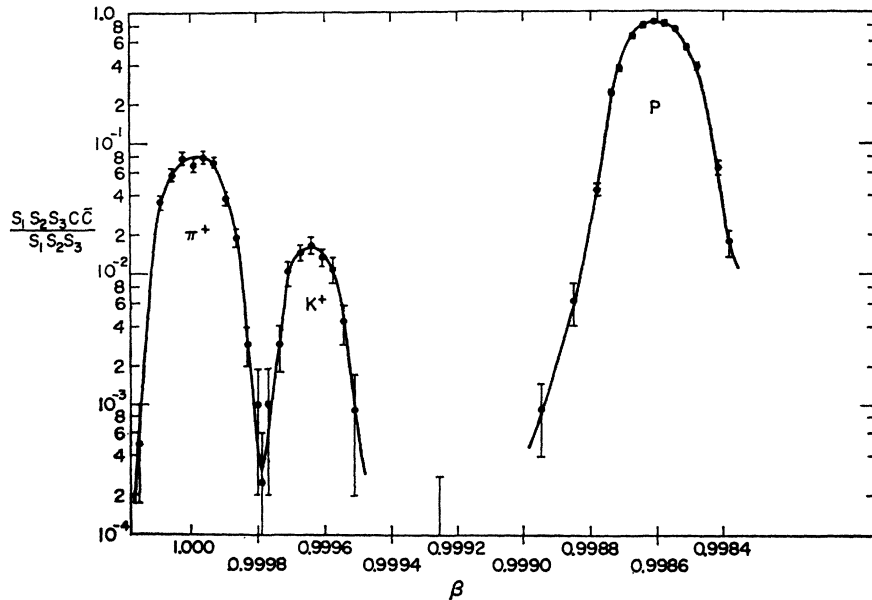


FIG. 4. Performance of Čerenkov counter at 18 BeV/c. This curve was taken by varying the gas pressure and measuring the fraction of the beam counted by the Čerenkov counter.

in the instantaneous counting rates. For this reason, an additional coincidence channel was provided to record ($S_1 S_2 S_3 C \bar{C}$) (S_6 delayed) where the delay inserted in the S_6 channel was 217 nsec which corresponded to the time difference between successive rf beam bunches within the accelerator. In this way the accidental coincidence rate could be continuously monitored and an accurate correction made.

An auxiliary 1-in.-diam counter S_7 was placed just behind S_6 . It could be moved by remote control horizontally or vertically in a plane perpendicular to the beam axis. Coincidences ($S_1 S_2 S_3 C C S_7$) were then used

for beam alignment and for measuring the size of the focal spot of the beam. Similarly, the coincidence ($S_1 S_2 S_3 C \bar{C} S_4 S_7$) was used to check periodically the efficiency of counter S_i for $i=4, 5$, and 6. The measured efficiency of the counters and their associated electronic circuits was greater than 99%.

D. Hydrogen Target

The hydrogen target was 120 in. long and 11 in. in diameter. The windows at each end of the target were 1.42 g cm^{-2} Al; the hydrogen was 21.3 g cm^{-2} . A dummy target was used for target-empty runs.

III. EXPERIMENTAL PROCEDURE

The mean momentum values were obtained from the accurately measured integral field excitation curves¹⁹ of magnet D and the geometry of the apparatus. The values were checked by measuring the velocity of known particles with the Čerenkov counter C . The values of $\Delta p/p$ were obtained from calculations using the dimensions of the pertinent aperture stops.

The magnet currents required in the quadrupole lenses were calculated¹⁶ in advance for a suitable selection of momenta. Final adjustments of the currents in quadrupoles Q_1 and Q_2 were made by maximizing the efficiency of the counter C at a few momenta. Thereafter these currents could be set satisfactorily by scaling with the measured magnet excitation curves.¹⁹ The final adjustment of Q_3 and Q_4 was made at a few points by measuring directly the size of the focal spot with counter S_7 (see Sec. II C). Thereafter, a satisfactory procedure was found to be an adjustment of currents at each

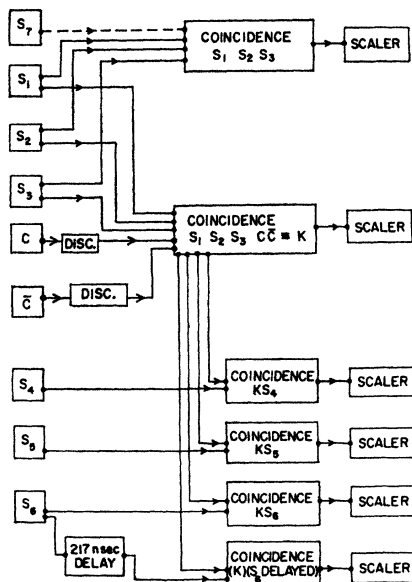


FIG. 5. Block diagram of the electronics.

¹⁹ G. T. Danby, Brookhaven National Laboratory Accelerator Department Internal Report GTD-2 (unpublished).

TABLE I. Total cross sections for K^+ on protons. The magnitude of the included corrections are listed explicitly.

Momentum (BeV/c)	σ uncorrected, large counter	$\Delta\sigma$, diffraction extrapolation	$\Delta\sigma$, beam contamination	$\Delta\sigma$, Coulomb scattering	σ_{Total} (mb)
3.25	20.4±0.5 ^a	0.3±0.1	-1.1±0.4	-2.1±1.0	17.5±1.2
4.0	19.0±0.7 ^a	0.5±0.4	-0.6±0.6	-1.3±0.6	17.6±1.2
5.5	17.4±0.5 ^a	1.0±0.5	-0.1±0.1	-0.4±0.2	17.9±0.8
7.0	16.8±0.4	1.8±0.3	-0.1±0.1	-0.1±0.1	18.4±0.6
8.5	17.2±0.4	1.8±0.3	-0.3±0.2	0±0	18.7±0.6
10.0	17.4±0.4	2.0±0.4	-0.6±0.4	0±0	18.8±0.7
10.9	17.8±0.3	1.0±0.4	-0.7±0.4	0±0	18.1±0.7
11.5	16.6±0.4	2.6±0.4	-0.2±0.2	0±0	19.0±0.6
12.5	16.1±0.4	2.5±0.7	-0.3±0.2	0±0	18.3±0.8
13.4	16.5±0.3	1.8±0.3	-0.8±0.4	0±0	17.5±0.6
15.0	17.9±0.5	1.3±0.4	-0.7±0.3	0±0	18.5±0.7
16.9	17.5±0.3	1.9±0.3	-0.6±0.4	0±0	18.8±0.6
19.0	17.3±0.4	1.3±0.3	-1.3±0.7	0±0	17.3±0.9

^a Corrected additionally (0.4, 0.2, 0.1 mb) for target in, out decay rate difference.

momentum value to give maximum efficiency for the coincidence ($S_1S_2S_3CCS_4$) with the dummy target in place. The focal spot, for example at 14.5 BeV/c, was approximately 1.25 in.×2.25 in.

After all magnets had been adjusted, a curve of the ratio ($S_1S_2S_3CC$)/($S_1S_2S_3$) versus the pressure in counter C was made at each momentum and the operating point selected. At each momentum, a measurement consisted of several runs, alternating target and dummy target in the beam.

IV. RESULTS

The cross section as measured by each of the three final counters (S_4 , S_5 , and S_6) was computed from the counting rates recorded with the target in place and those with the dummy target. A correction for accidental coincidences, which were continuously monitored (see Sec. II C), was applied; this correction was always less than 2%.

In addition to the correction for accidental coincidences, several other corrections must be applied to obtain the final value of the total cross section. These corrections are described below and their values are given in Tables I and II.

A. Beam Contamination

Since the pressure curves of counter C (see Fig. 4) do not fall to zero above and below the K -meson peak, the particles selected by counter C contain a small contamination of particles other than K mesons. The value of this correction depends upon the fractional contamination which is estimated from the peak-to-valley ratio of the pressure curve, and upon the difference in the cross section of the K mesons and the beam contaminant. The effective cross section of the contaminant has been obtained in two ways; either by direct measurement with the counter C set at the valley pressure, or by assuming, in agreement with the direct measurements, that the contamination corresponds to that of the principal beam component.

B. Decay in Flight

The K mesons lose more energy in the filled hydrogen target than in the dummy target. For this reason, with hydrogen in place, more of them decay between the target and the final counters. This correction is only 0.4 mb at the lowest momentum and is negligible for momenta above 5.5 BeV/c.

TABLE II. Total cross sections for K^- on protons. The magnitude of the included corrections are listed explicitly.

Momentum (BeV/c)	σ uncorrected, large counter	$\Delta\sigma$, diffraction extrapolation	$\Delta\sigma$, beam contamination	$\Delta\sigma$, Coulomb scattering	σ_{Total} (mb)
4.0	29.0±1.8 ^a	0.5±0.3	0.0±0.2	-1.3±0.6	28.2±1.9
5.5	23.8±0.7 ^a	1.0±0.3	-0.1±0.1	-0.4±0.2	24.3±0.8
7.0	23.3±0.4	1.8±0.3	0±0	-0.1±0.1	25.0±0.5
8.5	23.1±0.7	1.5±0.3	0±0	0±0	24.6±0.8
10.0	21.3±0.6	2.0±0.4	-0.1±0.1	0±0	23.2±0.7
11.5	19.5±0.5	3.8±0.6	0±0	0±0	23.3±0.8
12.0	22.0±0.6	1.0±0.4	-0.1±0.1	0±0	22.9±0.7
13.4	19.6±0.4	2.1±0.5	-0.2±0.1	0±0	21.5±0.7
14.5	19.9±0.6	1.9±0.5	-0.2±0.1	0±0	21.6±0.8
15.8	20.5±0.7	1.8±0.3	-0.4±0.2	0±0	21.9±0.8
17.5	20.6±0.7	1.7±0.5	-0.4±0.2	0±0	21.9±0.8
19.1	19.1±1.5	3.0±0.6	-0.5±0.4	0±0	21.6±1.7

^a Corrected additionally (0.2, 0.1 mb) for target in, out decay rate difference.

C. Coulomb Scattering

The sizes of the counters S_4 , S_5 , and S_6 were chosen such that the loss of beam due to multiple Coulomb scattering within the target could be neglected except at momenta of 7 BeV/c and below. Corrections to the low momentum points were made using the method and curves given by Sternheimer.²⁰ The unscattered beam distribution required to apply this method was measured by the transmission counters with the dummy target in place.

D. Extrapolation to Zero Angle

Although the beam and final counters were designed to present the minimum solid angle, a small correction must be made to the measured cross sections to take into account collisions in which one or more particles fall within the smallest counter. It is expected that the small-angle elastic scattering will give the major contribution to this correction. We assume that the forward scattering can be adequately described by an optical model, namely, that for small angles

$$\int_0^\theta \frac{d\sigma}{d\Omega} d\Omega = ar^2(p \sin\theta)^2, \quad (1)$$

where a is a constant, r is the proton radius, p is the momentum, and θ is the half-angle subtended by the final counter. The correction is then obtained by plotting the cross sections as measured by the three final counters S_4 , S_5 , and S_6 as a function of $(p \sin\theta)^2$ and extrapolating to zero angle. An example of this plot is shown in Fig. 6.

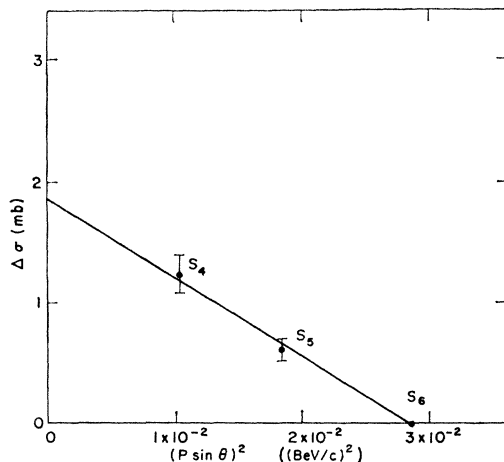


FIG. 6. Diffraction scattering extrapolation for K^+ mesons at 16.9 BeV/c. Errors are taken with respect to the largest counter, S_6 . The extrapolation is made to zero solid angle to find the total correction for diffraction scattering. The smallest counter, S_4 , was made large enough not to include Coulomb scattering in its measurement of the cross section.

If the integrated elastic cross section were known, the "optical" radius could be deduced from the slope of this curve. Unfortunately, these data are not available. If we assume that the elastic cross section is, for example, equal to one-fourth of the total cross section, we deduce a radius of 1.1 ± 0.2 F. This value is in accord with the data on high-energy pion scattering, which leads us to believe that our procedure is adequate to obtain the desired corrections.

At 7 BeV/c and below, the contribution from multiple Coulomb scattering in the smallest counter was appreciable so that the extrapolation was less certain. For these cases, we have assumed that the slope of the extrapolation was the same as that obtained at the higher momenta and have made the correction accordingly.

The final corrected total cross-section values obtained in this experiment are given in Tables I and II and are displayed in Fig. 7. Figures 8 and 9 give a comparison of our data with those obtained in other experiments.

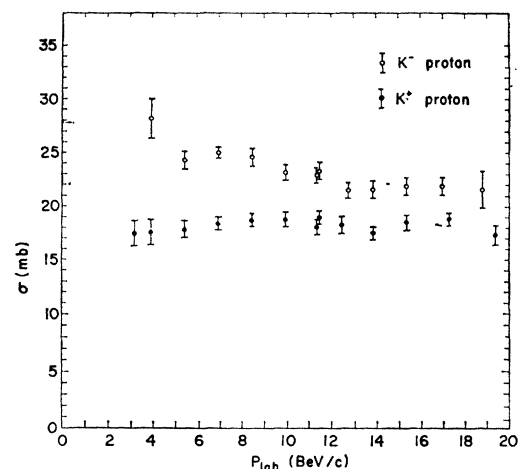


FIG. 7. K^+ - p and K^- - p total cross sections measured in this experiment.

V. DISCUSSION OF RESULTS

Our data for the K^+ total cross sections show no significant variation with momentum from 3.25 to 19.0 BeV/c. Over the entire range, a constant cross section of 18.4 mb gives an excellent fit to the measured values.

Figure 8 shows that there are important disagreements in the published K^+ data below 5 BeV/c. Our measurements appear to connect smoothly to those reported by Cook *et al.*⁷ and by Vovenko *et al.*⁶ at lower momenta. The increase in cross section below 4 BeV/c reported by Von Dardel *et al.*^{9,10} is not confirmed by our results, although our data agree with their measurements above 4 BeV/c.

Our measurements show a slowly decreasing K^- total cross section between 4 and 19 BeV/c. The values at all momenta are significantly higher than those for

²⁰ R. M. Sternheimer, Rev. Sci. Instr. 25, 1070 (1954).

K^+ ; the $K^- - K^+$ difference decreases from about 8 mb at 5 BeV/c to approximately 3 mb at 19 BeV/c.

Below 5 BeV/c, Fig. 9 shows some disagreements between the values given by various authors. However, the reported errors are such that these variations do not seem particularly significant. Our results and those of Von Dardel *et al.* again agree above 5 BeV/c.

Since there remains an appreciable difference between the K^+ and K^- cross sections up to the highest momenta, it is clear that these data cannot confirm the Pomernchuk limit theorem. Similar results have been previously reported for $\sigma_i(\pi^\pm p)$, $\sigma_i(p p)$, and $\sigma_i(\bar{p} p)$.²¹⁻²³

Attempts have been made to fit the data above 5 BeV/c to functional forms suggested by the Regge pole theory. When applied to the sum $\sigma_i(K^- p) + \sigma_i(K^+ p)$, two poles, one of which is the vacuum pole, are expected

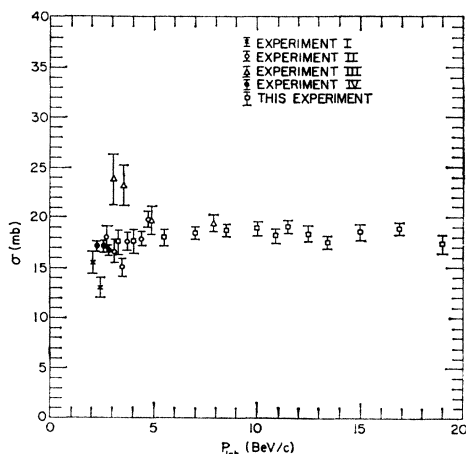


FIG. 8. Comparison of $K^+ - p$ total cross sections with previous experiments. Experiment I: H. C. Burrowes *et al.* reference 5. Experiment II: A. S. Vovenko *et al.* (reference 6). Experiment III: G. von Dardel *et al.* (reference 9) Experiment IV: V. Cook *et al.* (reference 7).

to give appreciable contributions.¹⁴ In this case, the sum is expected to take the simple form $a + b/E^{1-\alpha(0)}$, where a , b , and $\alpha(0)$ are constants independent of energy and E is the total energy of the incident particle in the laboratory system. It is interesting to note that we observe $\sigma_i(K^+ p)$ to be constant within errors. Thus, the contributions of the several trajectories other than the vacuum must be small or their contributions must cancel out nearly exactly. The following forms were therefore selected for fitting to the data: $\sigma_i(K^+ p) = A$ and $\sigma_i(K^- p) = A + B/E^{1-\alpha(0)}$. The best fit to the

²¹ S. J. Lindenbaum, W. A. Love, J. A. Niederer, S. Ozaki, J. J. Russell, and L. C. L. Yuan, Phys. Rev. Letters 7, 185 (1961).

²² S. J. Lindenbaum, W. A. Love, J. A. Niederer, S. Ozaki, J. J. Russell, and L. C. L. Yuan, Phys. Rev. Letters 7, 352 (1961).

²³ G. von Dardel, D. Dekkers, R. Mermod, M. Vivargent, G. Weber, and K. Winter, Phys. Rev. Letters 8, 173 (1962).

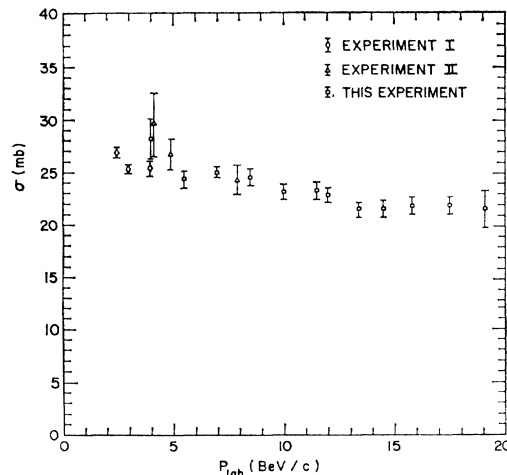


FIG. 9. Comparison of $K^- - p$ total cross sections with previous experiments. Experiment I: V. Cook *et al.* (reference 8). Experiment II: G. von Dardel *et al.* (reference 9).

data gives $A = 18.4 \pm 0.2$ mb, $B = 21.7 \pm 6.2$, and $\alpha(0) = 0.36 \pm 0.13$.

The second pole, $\alpha(0)$, which contributes to the sum $\sigma_i(K^- p) + \sigma_i(K^+ p)$ has the quantum numbers of the vacuum. If $\alpha(0)$ is on the ABC trajectory,²⁴ then this trajectory falls from $\alpha = 0.36$ at $t = 0$ to $\alpha = 0$ at $t = M_{ABC}$. In this case the ABC would not be a true resonance. Alternatively, $\alpha(0)$ could correspond to another vacuum trajectory, p' , proposed by Igi²⁵ who has shown that $0 < \alpha_{p'}(0) < 1$.

Very little can be learned from attempts to interpret the cross section difference $\sigma_i(K^- p) - \sigma_i(K^+ p)$. In this case the theory suggests too many constants to be determined, and the data are not sufficiently accurate to determine them unambiguously.

It should also be remarked that although the data are consistent with a monotonic energy variation, they do not constitute strong evidence against the possible presence of resonances. Not only are the measured values widely spaced in momentum, but also the amplitude to be expected for resonances, if any, in a single state of angular momentum would be small at these energies.

ACKNOWLEDGMENTS

It is a pleasure to acknowledge the assistance and cooperation of the members of the AGS Department. We wish also to thank George Munoz, Oscar Thomas, Thomas Conaway, and K. Wendell Chen for their technical assistance during this experiment.

²⁴ The ABC pole refers to the $I = 0$ two-pion anomaly observed by Abashian, Booth, and Crowe near threshold of $\pi - \pi$ scattering [N. E. Booth, A. Abashian, and K. M. Crowe, Phys. Rev. Letters 7, 35 (1961)].

²⁵ K. Igi, Phys. Rev. Letters 9, 76 (1962). The p' trajectory has been applied to a fitting of $p - p$ and $\bar{p} - p$ scattering by F. Hadjiioannou, R. J. N. Phillips, and W. Rarita, *ibid.* 9, 183 (1962).